

# Synthesis of Curcumin-Loaded Complex Coacervate of Chitosan Phosphate and Sodium Alginate and Study of their Antibacterial Activity

Arunima Sarma<sup>1</sup>, Chayanika Deka<sup>1</sup>, Sashi Prava Devi<sup>2</sup>, Dilip Kumar Kakati<sup>1,\*</sup>

<sup>1</sup>Department of Chemistry, Gauhati University, Guwahati, Assam, INDIA.

<sup>2</sup>Department of Botany, Gauhati University, Guwahati, Assam, INDIA.

## ABSTRACT

**Background:** In a system of two oppositely charged colloids a spontaneous liquid-liquid phase separation is termed as complex coacervation and the separated phase is called coacervate. In recent times coacervates prepared from different colloidal systems have found extensive uses in the microencapsulation of bioactive molecules including drugs. The search for new coacervation systems and coacervates with novel properties remains an active area of research. In the present work preparation of complex coacervate from chitosan phosphate and sodium alginate for subsequent use for encapsulation of curcumin is reported. **Materials and Methods:** Chitosan was first modified to chitosan phosphate. It was then reacted with sodium alginate to form the complex coacervate. Several parameters like ratio of concentration of the chitosan phosphate to alginate, pH of the reaction media were varied to attain the optimum condition for the maximum yield of the coacervate. **Results:** It was found that the maximum amount of coacervate formed at pH 3.6 and at the ratio of 5:4 by volume of the 3% solution of alginate and chitosan phosphate. The maximum loading efficiency of curcumin was found to be 84%. Swelling and release studies were carried out at different pH and the maximum swelling and percentage of release was observed at pH 9. The curcumin loaded coacervate showed mild antibacterial activity against *Staphylococcus aureus*, *Bacillus subtilis* and *Enterobacter aerogenes*. **Conclusion:** Results from Fourier transform infrared spectroscopy, thermogravimetric analysis, powder x-ray diffraction and scanning electron microscopy supported successful encapsulation of curcumin in the chitosan phosphate/alginate coacervate. Swelling and release studies could be modulated by changing the pH of the medium. A sustained release behavior of curcumin over a period of 72 hr was observed without the loss of physical integrity of the coacervate.

**Keywords:** Curcumin, Chitosan Phosphate, Sodium Alginate, *Staphylococcus aureus*, *Bacillus subtilis*, *Klebsiella pneumonia*, *Enterobacter aerogenes*.

## Correspondence:

Prof. Dilip Kumar Kakati

Department of Chemistry, Gauhati University, Guwahati-781014, Assam, INDIA.

Email: dkk.chem@gauhati.ac.in

**Received:** 24-05-2023;

**Revised:** 23-09-2023;

**Accepted:** 12-02-2024.

## INTRODUCTION

Curcumin is a naturally available bioactive molecule and has been in use in traditional medicine for hundreds of years.<sup>1,2</sup> The yellow colour of turmeric, isolated from the rhizome of *Curcuma longa* is due to curcumin which constitutes about 77 weight percent of turmeric.<sup>3</sup> Curcumin has significant anti-inflammatory, anti-infective, anti-oxidant,<sup>4</sup> anti-mutagenic, anti-microbial,<sup>5</sup> anti-carcinogenic,<sup>6</sup> anticoagulant and wound healing properties.<sup>7-13</sup> However the potential use of curcumin as a drug is handicapped by its properties such as aqueous insolubility, rapid metabolism and instability in biological

systems. All these properties result in poor bioavailability of curcumin when used as a drug. To overcome these problems and increase the bioavailability of curcumin several strategies have been explored. These mainly constitute the encapsulation in liposomes and polymeric micellar systems, cyclodextrin based inclusion complex and formation of curcumin cocrytals<sup>14</sup> with other compounds. Complex coacervate is another medium of choice for encapsulation, protection and delivery of bioactive molecules including curcumin<sup>15,16</sup> Complex coacervate results from electrostatic interaction between two oppositely charged colloids in a system. As such wide variety of oppositely charged biopolymers like proteins and polysachharides are potential precursors for formation of coacervates. Mohammadian *et al.*<sup>17</sup> reported the use of gum *Arabic* and whey protein nano fibrils based complex coacervates as medium for encapsulation of curcumin. A complex coacervate from gum *Arabic* and albumin was used by Shahgholian and others<sup>18</sup> for encapsulating curcumin



DOI: 10.5530/ijper.58.2s.45

### Copyright Information :

Copyright Author (s) 2024 Distributed under Creative Commons CC-BY 4.0

Publishing Partner : EManuscript Tech. [www.emanuscript.in]

and the encapsulation efficiency was reported to be 92%. Complex coacervates based on gum *Arabic* and chitosan,<sup>19</sup> ovalbumin and k-carragenan<sup>20</sup> were also used as medium for encapsulation and delivery of curcumin. Huang et al.<sup>21</sup> developed a system based on lysozyme and k-carragenan as a delivery vehicle for curcumin.

The present work describes the encapsulation and release behavior of curcumin in a complex coacervate prepared from chitosan phosphate having a better aqueous solubility than chitosan itself and sodium alginate. Antibacterial activity of curcumin loaded coacervate was investigated against four different bacterial strains, 2 g positive (*S. aureus* and *B. subtilis*) and 2 g negative (*K. pneumoniae* and *E. aerogenes*).

## MATERIALS AND METHODS

### Materials

75-85% deacetylated chitosan of low molecular weight (Sigma-Aldrich, India), curcumin (Sigma-Aldrich, India), sodium alginate (Himedia Laboratories, India), ethanol, DMSO (Merck, India), were used without further purification. Inhibition zone scale and nutrient broth were procured from Himedia, India. Four bacterial strains *S. aureus* (MTCC No. 737), *B. subtilis* (MTCC No. 736), *K. pneumoniae* (MTCC No. 619) and *E. aerogenes* (MTCC No. 111) used in the investigation were procured from MTCC, Chandigarh. All experiments were carried out in deionized water.

### Methods

#### Preparation of Chitosan Phosphate

In a three necked flask fitted with a thermometer, water condenser and nitrogen gas inlet, 2 g chitosan, 6 g orthophosphoric acid and 100 mL 2% acetic acid were mixed.<sup>22</sup> The reaction mixture was heated to dissolve chitosan and then refluxed for 2 hr. The resultant solution was cooled and then poured in excess methanol. The heavy white precipitate formed was dissolved in minimum volume of deionized water and reprecipitated in excess methanol. The precipitate, chitosan phosphate, was dried in a vacuum oven at 80°C.

#### Optimization of reaction conditions for the preparation of coacervate

Two parameters, the pH of the reaction medium and the relative ratio of the concentration of the two constituents of the complex coacervate were changed to obtain the optimum condition for the maximum yield of the complex coacervate.

#### Determination of optimum pH of the reaction medium

Buffer solutions of ten different pH (3.2, 3.6, 3.8, 4.0, 4.2, 4.4, 4.6, 4.8, 5.0, and 5.2) were prepared from 0.1N acetic acid and

0.1N sodium acetate solution. 3% (w/v) solutions of sodium alginate and chitosan phosphate were prepared separately in 100 mL buffer solution of specific pH. Sodium alginate solution was added drop wise to chitosan phosphate solution under stirring at room temperature. The procedure was followed for buffer solutions of ten different pH. The coacervate formed was dried in vacuum oven at 40°C till constant weight was obtained.

#### Determination of optimum ratio of chitosan phosphate to sodium alginate

Optimum ratio of the two components was determined at pH 3.6 of the reaction medium. 0.3% (w/v) solutions of sodium alginate and chitosan phosphate were prepared separately in buffer solution of pH 3.6. Chitosan phosphate and sodium alginate solutions were mixed at eight different volume ratios at room temperature, keeping the total volume of the mixture at 45 mL. Different volume ratios of sodium alginate: chitosan phosphate were 40:5, 35:10, 30:15, 25:20, 20:25, 15:30, 10:35, 5:40 respectively. The optimum ratio of the two components resulting in maximum yield of complex coacervate was determined by measuring weights of the coacervate formed, and also by measuring the viscosity, UV-absorbance (UV-1800, SHIMADZU) and conductivity of the supernatant liquid.

#### Swelling Studies

Swelling behavior of the coacervate was investigated at pH 4, 7, 7.4 (phosphate buffered saline system) and 9. The weights of four samples of the dry coacervates were measured and then immersed in solutions of four different pH. The weights of the swollen coacervates were measured at fixed intervals of time up to a limit of 72 hr. The equilibrium swelling index was calculated from the relationship:

$$\text{Swelling Index (\%)} = \left[ \frac{W_g - W_o}{W_o} \right] \times 100$$

Where, weight of dry coacervate =  $W_o$  and weight of swelled coacervate =  $W_g$ .

#### Preparation of curcumin loaded chitosan phosphate/sodium alginate coacervate

Curcumin loaded coacervates were prepared at pH 3.6 and volume ratio of 3% solution of sodium alginate to chitosan phosphate at 5:4. A 0.3% (w/v) solution of sodium alginate was prepared in 250 mL buffer of pH 3.6. Curcumin solutions containing varying weight (0.05-2.0) g were prepared in 100 mL ethanol. A 0.3% (w/v) solution of chitosan phosphate was also prepared in 250 mL buffer of pH 3.6. To this solution of chitosan phosphate, ethanolic solution of curcumin was added drop wise. This was followed by the drop wise addition of alginate solution. After complete addition, the reaction mixture was stirred for 1h followed by removal of ethanol. The resultant product was then freeze dried.

### Preparation of calibration curve for curcumin

A known amount of curcumin was dissolved in 100 mL ethanol and a series of dilute solutions were prepared from this stock solution. The absorptions at 427 nm were recorded in a UV-visible spectrophotometer (UV-1800, SHIMADZU). On plotting the absorbance values at 427 nm against the concentration of the curcumin solutions, a straight line was obtained with the following characteristics,  $y=1455x+0.0138$  and  $R^2=0.9956$  which is shown in Figure 3(i).

### Loading Efficiency (LE)

The curcumin loaded into the coacervates was extracted by agitating in ethanol for half an hour. The curcumin thus extracted was quantified from its absorbance at 427 nm from the calibration curve. The loading efficiency of curcumin was derived from the following relation:

$$LE(\%) = \frac{\text{Total amount of curcumin loaded in the coacervate}}{\text{Total amount of curcumin taken}} \times 100$$

Loading efficiencies were determined at varying amounts of curcumin in the loading solution.

### Release studies

The release of curcumin from loaded coacervate was investigated in medium of pH 4, 7, 9 and 7.4 (phosphate buffered saline) over a period of 72 hr. The weighed samples of loaded coacervates were placed in seven tubes containing a medium of definite pH. After fixed interval of time the content of the tubes were centrifuged and the UV spectra were recorded for the supernatant liquid. The amount of curcumin released was determined from the calibration curve. The percentage of curcumin released was determined from the following relation.<sup>23</sup>

$$\text{Release}(\%) = \frac{\text{Released curcumin from the coacervate}}{\text{Total amount of curcumin in the coacervate}} \times 100$$

### Antibacterial activity assay

The antibacterial activity of curcumin loaded coacervate was investigated against four different bacterial strains: 2 g positive (*S. aureus* and *B. subtilis*) and 2 g negative (*K. pneumoniae* and *E. aerogenes*) by agar well diffusion method. The organisms were cultured in nutrient broth for 24-48 hr. Erythromycin antibiotic disc and DMSO disc were used as positive and negative controls respectively.

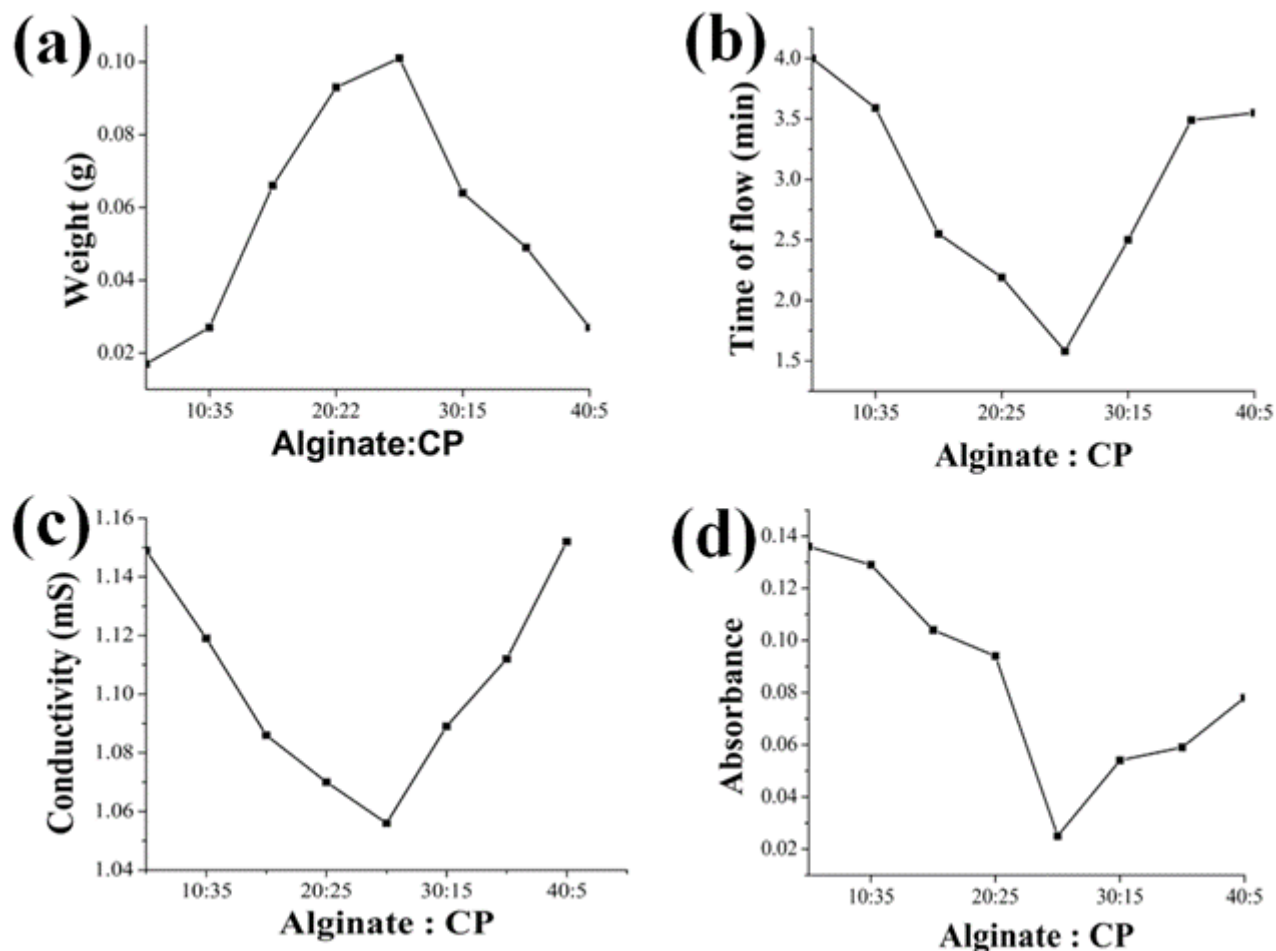


**Figure 1:** Alginate: Chitosan phosphate ratio by volume against (a) weight of coacervate formed (b) viscosity (time of flow) of the supernatant liquid (c) conductivity of the supernatant liquid (d) UV-absorbance at 250 nm of the supernatant liquid.

## RESULTS

### Preparation of coacervate: Optimization of reaction parameters

The pH of the reaction medium giving the maximum yield of the coacervate was found to be 3.6. The relative ratio of concentration of alginate to chitosan phosphate giving the maximum yield at pH 3.6, was determined and the results are shown in Figure 1. The results showed the most suitable ratio of 3% solution of alginate to chitosan phosphate by volume as 5:4.

### FTIR study

The FTIR spectra of chitosan, chitosan phosphate, alginate, coacervate, curcumin and curcumin loaded coacervate are shown in Figure 2(i) and (ii). A SHIMADZU IR Affinity-1 FTIR spectrophotometer, with a scanning range of 4000-400  $\text{cm}^{-1}$  was used to record the FTIR spectra in the form of KBr pellets. Data were recorded in the transmittance mode.

Chitosan showed peaks at 3462, 1643, 1554, 1415 and 1078  $\text{cm}^{-1}$ . The peak at 3462  $\text{cm}^{-1}$  is due to -OH stretching. Peak at 1643  $\text{cm}^{-1}$  is due to C=O stretching (amide I), peak at 1554  $\text{cm}^{-1}$  is due to N-H bending (amide II) and peak at 1415  $\text{cm}^{-1}$  is due to C-N stretching (amide III) and the peak at 1078  $\text{cm}^{-1}$  is due to C-O-C stretching.<sup>24,25</sup>

Alginate showed peaks at 3446, 1629, 1309, 1091, 1028 and 945  $\text{cm}^{-1}$ . The peak at 3446  $\text{cm}^{-1}$  is due to stretching vibrations of O-H bonds. The peak at 1629  $\text{cm}^{-1}$  is due to asymmetric stretching of O-C-O vibration of carboxylate salt ion while the peak at 1309  $\text{cm}^{-1}$  is due to C-C-H and O-C-H deformation. The peak at 1091  $\text{cm}^{-1}$  is due to C-O and C-C stretching vibration of pyranose rings and the peak at 1028  $\text{cm}^{-1}$  is due to C-O stretching vibration. The

peak at 945  $\text{cm}^{-1}$  is due to C-O stretching vibration of uronic acid residues.<sup>26</sup>

Chitosan Phosphate showed peaks at 3473, 1645, 1550, 1309, 1078 and 520  $\text{cm}^{-1}$ . The peak at 3473  $\text{cm}^{-1}$  is due to -OH group, the peaks at 1645  $\text{cm}^{-1}$  (amide I) and 1550  $\text{cm}^{-1}$  (amide II) are due to asymmetric and symmetric N-H bending respectively, the peak at 1309  $\text{cm}^{-1}$  is due to P=O stretching of phosphate group, the peak at 1078  $\text{cm}^{-1}$  is due to phosphorylated hydroxyl groups, the peak at 520  $\text{cm}^{-1}$  is due to P-OH group.<sup>27</sup>

The coacervate showed peaks at 3454, 1649, 1554, 1421 and 524  $\text{cm}^{-1}$ . Most of the peaks due to chitosan phosphate and the alginate are present in the coacervate with small variation in the absorption values. The peaks due to amide-I and amide-II moves to longer wavelength due to protonation of the  $\text{NH}_2$  group in chitosan phosphate and electrostatic interaction with alginate

Curcumin showed peaks at 3479, 2362, 2337, 1629, 1564, 1425, 1278 and 964  $\text{cm}^{-1}$ . The peak at 3479  $\text{cm}^{-1}$  is due to O-H groups while the peaks due to asymmetric and symmetric stretching of methylene groups appeared at 2362  $\text{cm}^{-1}$  and 2337  $\text{cm}^{-1}$  respectively. The peaks at 1629  $\text{cm}^{-1}$  and 1564  $\text{cm}^{-1}$  are due to C=C vibration of olefinic group, while the peak at 1425  $\text{cm}^{-1}$  is due to C=C aromatic stretching vibration. The peak at 1278  $\text{cm}^{-1}$  is due to C-O stretching and the peak at 964  $\text{cm}^{-1}$  is due to out-of-plane vibration of aromatic C-C.<sup>22</sup>

Curcumin loaded coacervate showed peaks at 3449, 1637, 1560, 1429 and 879  $\text{cm}^{-1}$ . As is evident all the peaks of coacervate are present in the curcumin loaded coacervate as well with small shifts in the peak positions, which may be indicative of presence of in situ interactions between the coacervate and the curcumin. Further the additional peak at 879  $\text{cm}^{-1}$  present in the spectra, is due to the aromatic group in curcumin.

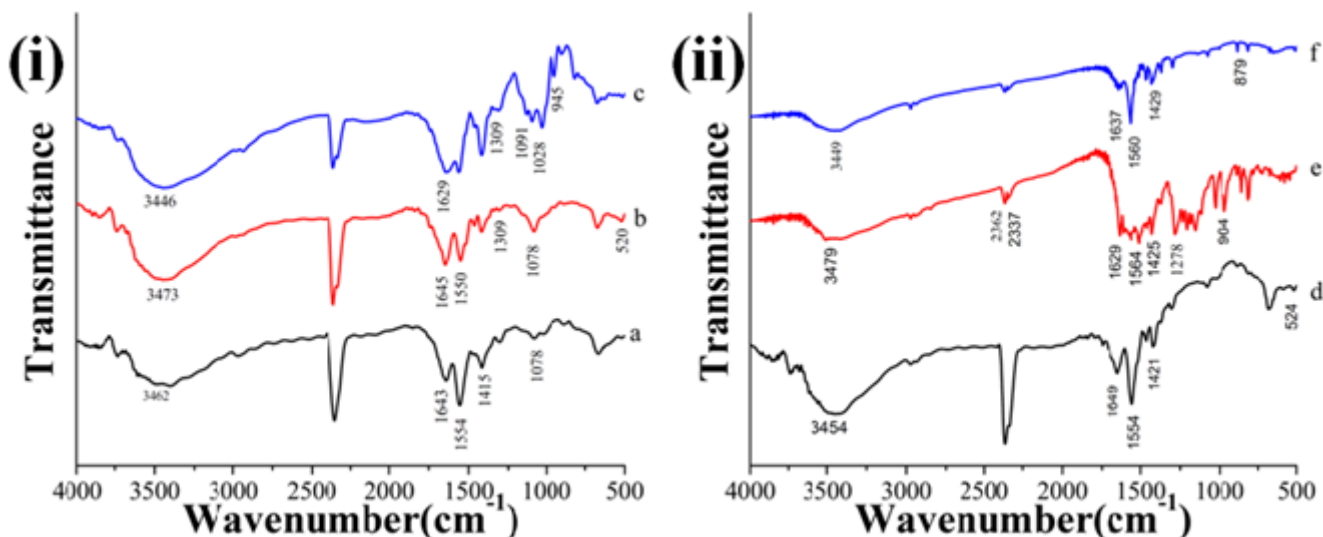


**Figure 2:** (i) FTIR spectra of (a) chitosan (b) chitosan phosphate (c) alginate. (ii) FTIR spectra of (d) coacervate (e) curcumin (f) curcumin loaded coacervate.



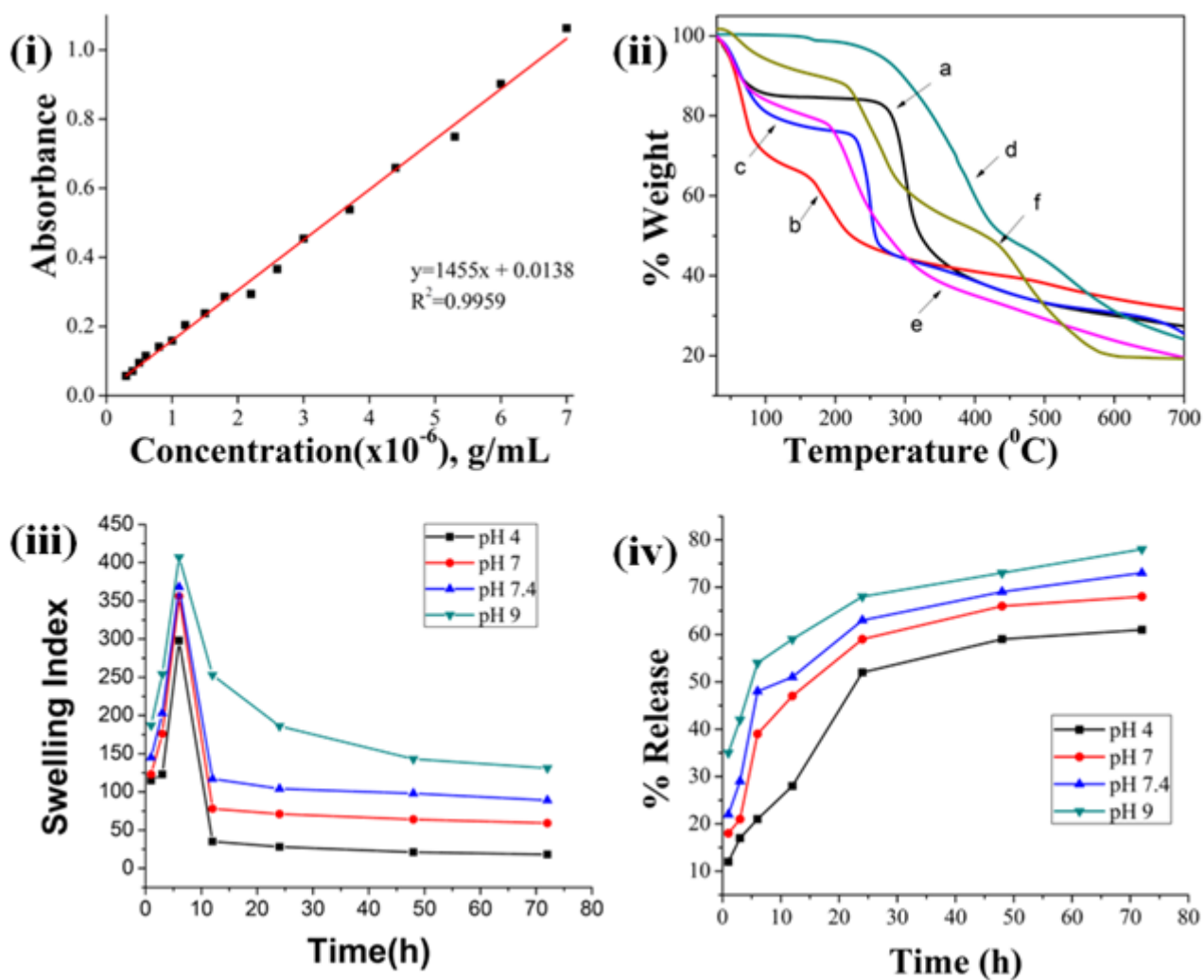


**Figure 3:** (i) Calibration curve of curcumin (ii) Thermogravimetric curves of (a) chitosan (b) chitosan phosphate (c) alginate (d) curcumin (e) coacervate (f) curcumin loaded coacervate (iii) Swelling index of the coacervate at pH 4, 7, 7.4 and 9 (iv) % release of curcumin from the curcumin loaded coacervate at pH 4, 7, 7.4 and 9.

### TGA study

The thermo gravimetric analyses were done in the temperature range, 30-700°C at a heating rate of 10°C/min under a nitrogen flow of 20 mL/min. The data were recorded in Perkin Elmer TGA 4000 instrument. The results of thermo gravimetric analysis are presented in Figure 3(ii).

A two step thermal degradation was observed in case of chitosan and the major weight loss occurred at 300°C.<sup>28</sup> The thermal degradation profile distinctly changed with the phosphorylation of chitosan and the major weight loss for chitosan phosphate occurred at around 200°C. Deka *et al.*<sup>22</sup> reported similar thermal behavior of chitosan and chitosan phosphate. The major weight loss was observed at around 270°C for alginate.<sup>29</sup> Curcumin showed the highest thermal stability with the major weight loss at around 400°C.<sup>22</sup> When the TGA-curve of the coacervate is compared with those of chitosan phosphate and alginate, it becomes obvious that the coacervate formation changed the thermal degradation behaviour and it is found to have an

intermediate thermal stability with respect to the constituents. Further, loading of curcumin again changed the thermal behavior of the complex coacervate, with a rise in the thermal stability of the curcumin loaded coacervate with respect to the pristine coacervate. Unlike the pristine coacervate, it exhibits a distinct two stage thermal degradation. The TGA-curves of neat and curcumin loaded coacervates indicate that the two materials are not identical.

### XRD study

X-ray diffractograms of curcumin, pristine coacervate and curcumin loaded coacervate are presented in Figure 4(a), (b) and (c) respectively. An x-ray diffractometer, model X'Pert Pro, make PANalytical was used to record the spectra with a scan rate of 0.02° 2 $\theta$ /s in the scan range from 2 $\theta$ =5 to 40°. The XRD patterns indicated the amorphous and crystalline nature of the coacervate and curcumin respectively. The amorphous nature of the coacervate changed on loading of curcumin in it. As the coacervate is present in larger amount many of the peaks of

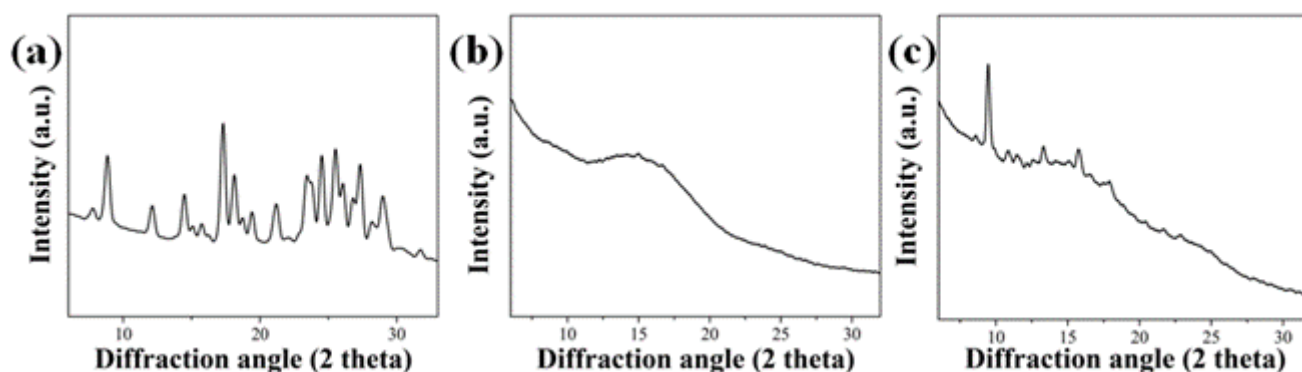


**Figure 4:** XRD pattern of (a) curcumin (b) coacervate (c) curcumin loaded coacervate.

**Table 1: Loading efficiency of the coacervate.**

| Amount of curcumin (g) in the loading solution | LE (%) |
|--|--------|
| 0.05   | 48     |
| 0.08   | 81     |
| 0.1  | 84     |
| 0.15   | 65     |
| 0.2  | 64     |

curcumin are masked. However, a few peaks at 9.46°, 13.30° and 15.76° for the curcumin appeared in the curcumin loaded coacervate, with marginal shifts in the 2 $\theta$  values of curcumin. This may be indicative of presence of some physico-chemical interactions between the matrix material and the curcumin.

### Swelling study

The swelling behaviour of the coacervates was followed by plotting the swelling index measured at four different pH against time and the resultant plots are presented in Figure 3(iii). From the plots it is evident that the swelling is dependent on the pH of the swelling medium. The highest and lowest swellings were observed at pH 9 and pH 4 respectively. Further a common pattern of swelling was observed at all pH. The swelling rate was very high in the initial hours and then it decreased and gradually attained an equilibrium value after approximately 10 h.

### Loading efficiency and Release Profiles

The result of investigation on loading efficiency of curcumin in the coacervate is presented in the Table 1. It is evident that the loading efficiency is dependent on the amount of the curcumin in the loading solution with a limiting amount of curcumin at which the loading attains a saturation value. A maximum loading efficiency of 84% was observed with curcumin 0.1 g in the loading solution.

Release of curcumin from the coacervate was studied at four different pH (4, 7, 7.4 and 9). The release of curcumin is pH dependent and the release behavior parallels the swelling

behavior. The plots of % of release against the time at the four different pH are presented in Figure 3 (iv). The % of release was maximum at pH 9 and minimum at pH 4. Further in all cases initial release was very fast and after approximately 25 h the % of release attains an equilibrium value and a slow and sustained release behavior is observed. Similar behavior was reported by Vandenberg *et al.*<sup>30</sup> and Zhang *et al.*<sup>31</sup> while studying the release of protein from chitosan-alginate microspheres.

### SEM study

A scanning electron microscope (Model Zeiss, SIGMA-300) operating at an accelerated voltage of 5 kV was used to record the SE-micrographs of pristine and curcumin loaded coacervates. The surfaces of the samples were coated with gold before SEM analysis. Scanning electron micrographs of the pristine and curcumin loaded coacervate are shown in Figure 5(i) and (ii). The loading of curcumin into the coacervate resulted in a distinct change in the morphology. The surface morphology changed from a smooth to a rugged one on encapsulation of curcumin as is visible from the micrographs.

### Antibacterial study

Table 2 shows the zone of inhibition of curcumin loaded coacervate against four different bacterial strains: 2 g positive (*S. aureus* and *B. subtilis*) and 2 g negative (*K. pneumoniae* and *E. aerogenes*). The curcumin loaded coacervate displayed antibacterial activity against both the gram positive bacteria and one of the gram negative bacteria (*E. aerogenes*). *E. aerogenes* (15 mm) showed the highest zone of inhibition. The unloaded coacervate showed no antibacterial activity against any of the gram positive and gram negative bacteria. In some cases DMSO exhibited moderate zone of inhibition. As the coacervates were dissolved in DMSO, zone of inhibition of coacervates were calculated by subtracting the zone of inhibition of DMSO. Figure 5(iii) shows the photoplates showing antibacterial activity of curcumin loaded coacervate against *S. aureus* (photoplate A), *B. subtilis* (photoplate B), *E. aerogenes* (photoplate C) and *K. pneumoniae* (photoplate D).

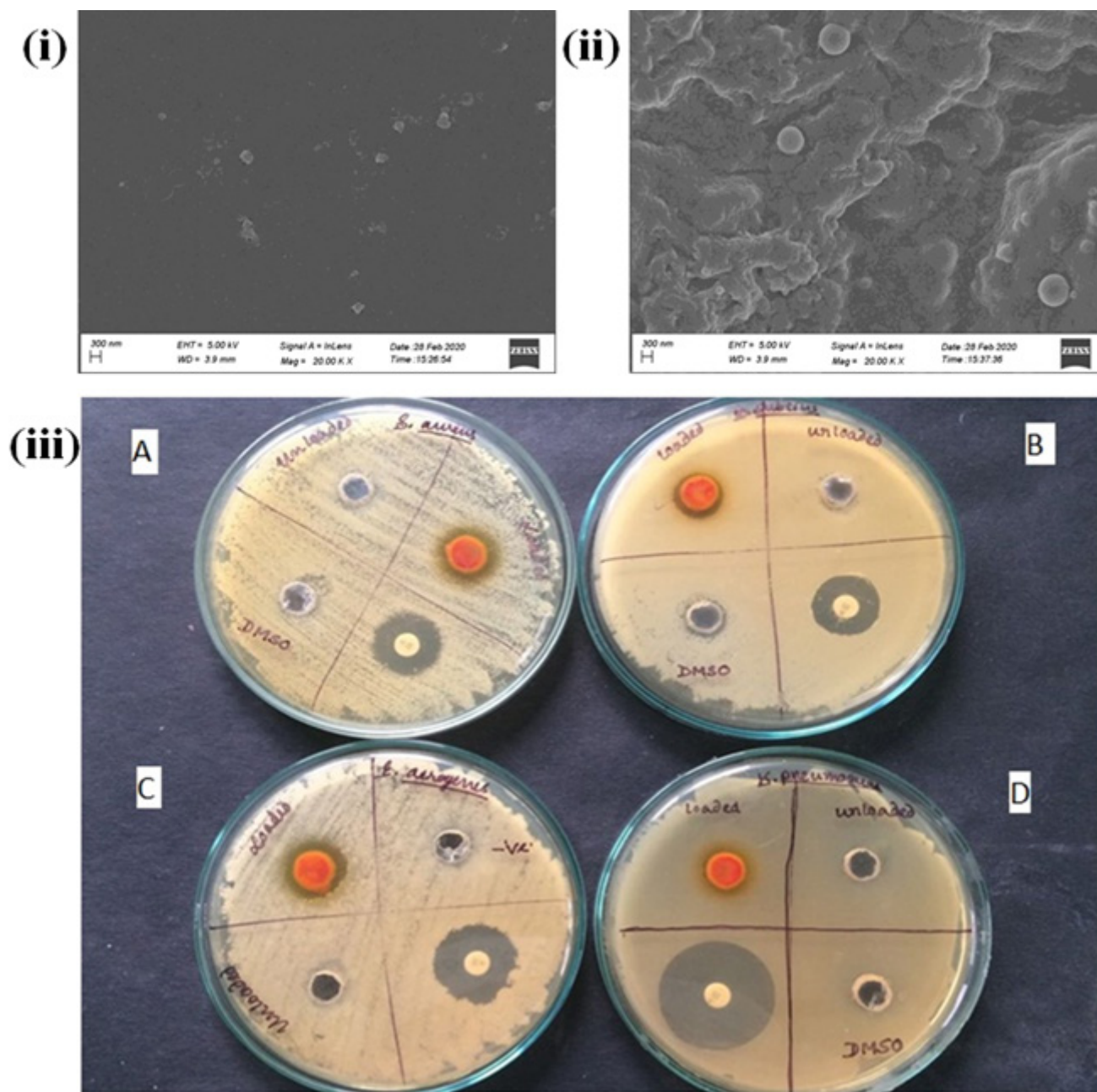


**Figure 5:** Scanning electron micrographs of (i)coacervate and (ii)curcumin loaded coacervate (iii) Photo plates showing antibacterial activity of curcumin loaded coacervate against *S. aureus*(A), *B. subtilis*(B), *E. aerogenes*(C) and *K. pneumoniae* (D).

## DISCUSSION

Curcumin possesses anti-inflammatory, anti-infective, anti-oxidant, anti-microbial and wound healing properties. In recent times curcumin is shown to have anti-cancer activities also. So it becomes essential to address two issues related to curcumin preventing its use as an effective drug, viz. low aqueous solubility and poor stability under physiological conditions. A complex coacervate prepared from chitosan phosphate and alginate is used to encapsulate curcumin to enhance its stability and facilitate slow and sustained release to remain effective for a longer period of time.

In the preparation of the coacervate, chitosan is modified to its phosphate to make it water soluble. The reaction parameters were varied to determine the optimum condition giving the maximum yield of the coacervate. The chitosan is protonated at acidic pH which enhances the electrostatic interaction with alginate leading to the higher yield of coacervate. The FTIR spectra indicated the formation of the coacervate from chitosan phosphate and alginate. The peaks of chitosan phosphate and alginate are found imprinted in the spectra of the coacervate. Further, the minor change in the absorption peak values of the chitosan phosphate and alginate in the coacervate indicated the presence of interaction between them through electrostatic



**Table 2: Zone of inhibition of curcumin loaded coacervate.**

| Microorganisms                | Types of microorganisms | Curcumin loaded coacervate (mm) | DMSO | Disk (mm) |
|-------------------------------|-------------------------|---------------------------------|------|-----------|
| <i>Staphylococcus aureus</i>  | Gram positive bacteria  | 14                              | -    | 18        |
| <i>Klebsiella pneumonia</i>   | Gram negative bacteria  | -                               | -    | 30        |
| <i>Enterobacter aerogenes</i> | Gram negative bacteria  | 15                              | -    | 20        |
| <i>Bacillus subtilis</i>      | Gram positive bacteria  | 12                              | -    | 18        |

interactions, hydrogen bonding etc. The TGA data besides being used to determine the range of thermal stability is also used for diagnostic purpose, as no two materials will have the same TGA curve. From that point of view, the TGA data also supported the formation of coacervate as well as the loading of curcumin in the coacervate. Similarly, the FESEM data also supported the successful encapsulation. The swelling studies at physiological pH as well as at acidic and alkaline pH indicated the robust nature of the coacervate as the physical integrity remains intact even after 72 h of swelling. Moreover the swelling was lowest at pH 4. At acidic pH chitosan phosphate is protonated resulting in strong bonding with alginate. The resultant tight network structure lowers the diffusion of water in to the coacervate structure<sup>32</sup>. However at elevated pH due to decreased protonation of chitosan phosphate the bonding is weakened resulting in the loosening of the network structure and facilitating higher degree of diffusion of water into the coacervate, resulting in increased swelling. The release pattern of curcumin from the coacervate as expected parallels the swelling pattern. Two observations can be made about the release behavior; firstly, it is pH dependent and highest at pH 9. And most importantly it showed a sustained release behavior over a period of 72 h, which is considered as a hallmark of a drug to remain effective for a longer period of time without causing any side effect. However at the initial period the release of curcumin is fast before attaining equilibrium, which may indicate that some portion of curcumin may remain adsorbed to the coacervate surface instead of being encapsulated inside the coacervate. The curcumin loaded coacervate showed antibacterial activity against three bacterial strains in *in vitro* test.

## CONCLUSION

A robust coacervate was prepared from chitosan phosphate and alginate, which maintained its physical integrity in solutions at four different pH 4, 7, 7.4 and 9 for up to a period of 72 h. The swelling is dependent on the pH of the medium and the maximum swelling was observed at pH 9. The curcumin was successfully loaded, by preparing the coacervate in presence of curcumin. The maximum loading efficiency attained was 84%. The FTIR, TGA, XRD and FESEM data supported the successful encapsulation of curcumin in the coacervate. The curcumin encapsulated in the coacervate gets released in a slow and sustained way in a pH dependent manner. Thus the dual issue which hinders the use of curcumin as a drug, i.e. poor bioavailability and inability to

remain effective for a prolonged period due to rapid metabolism under physiological conditions, could be suitably addressed by encapsulation in the coacervate from chitosan phosphate and sodium alginate. Further the curcumin loaded coacervate retains the antibacterial property of curcumin and found effective against three bacterial strains tested during the present investigation.

## ACKNOWLEDGEMENT

The authors gratefully acknowledge the FESEM service provided by the CIF, Gauhati University. Further, we thank DR Tridib Kumar Goswami, of the Department of Chemistry, for his valuable suggestions while preparing the manuscript.

## CONFLICT OF INTEREST

The authors declare no Conflict of interest.

## ABBREVIATIONS

MTCC: Microbial Type Culture Collection; FESEM: Field Emission Scanning Electron Microscopy; CIF: Central Instruments Facility.

## SUMMARY

A complex coacervate was prepared from two oppositely charged polysaccharides, Chitosan phosphate and alginate. Curcumin was loaded in the coacervate by preparing the coacervate in the presence of curcumin solution in ethanol. The neat coacervate and the curcumin-loaded coacervate were characterized by FTIR, TGA, XRD and FESEM studies. Swelling studies were carried out at four different pH, 4, 7, 7.4 and 9 and swelling was found to be dependent on the pH, with highest swelling at pH 9. The swelling was studied for a period of 72 hr and the coacervate maintained its integrity during that period. The release of curcumin from the curcumin loaded coacervate showed a sustained release behavior over a period of 72 hr. The curcumin loaded coacervate showed antibacterial property against three bacterial strains, *Staphylococcus aureus*, *Bacillus subtilis* and *Enterobacter aerogenes*.

## REFERENCES

- Li Y, Zhang T. Targeting cancer stem cells by curcumin and clinical applications. *Cancer Lett.* 2014; 346(2): 197-205. doi: 10.1016/j.canlet.2014.01.012.
- Esatbeyoglu T, Huebbe P, Ernst IMA, Chin D, Wagner AE, Rimbach G. Curcumin—from molecule to biological function. *Angew Chem Int Ed.* 2012; 51(22): 5308-32. doi: 10.1002/anie.201107724.
- Naksuriya O, Okonogi S, Schiffelers RM, Hennink WE. Curcumin nanoformulations: a review of pharmaceutical properties and preclinical studies and clinical data related



- to cancer treatment. *Biomaterials*. 2014; 35(10): 3365-83. doi: 10.1016/j.biomaterials.2013.12.090.
4. Basnet P, Skalko-Basnet N. Curcumin: an anti-inflammatory molecule from a curry spice on the path to cancer treatment. *Molecules*. 2011; 16(6): 4567-98. doi: 10.3390/molecules16064567.
  5. Fu X, Shen Y, Jiang X, Huang D, Yan Y. Chitosan derivatives with dual-antibacterial functional groups for antimicrobial finishing of cotton fabrics. *Carbohydr Polym*. 2011; 85(1): 221-7. doi: 10.1016/j.carbpol.2011.02.019.
  6. Aggarwal BB. Prostate cancer and curcumin: add spice to your life. *Cancer Biol Ther*. 2008; 7(9): 1436-40. doi: 10.4161/cbt.7.9.6659.
  7. Mohanty C, Das M, Sahoo SK. Sustained wound healing activity of curcumin loaded oleic acid based polymeric bandage in a rat model. *Mol Pharmaceutics*. 2012; 9(10): 2801-11. doi: 10.1021/mp300075u.
  8. Lim GP, Chu T, Yang F, Beech W, Frautschy SA, Cole GM. The curry spice curcumin reduces oxidative damage and amyloid pathology in an Alzheimer transgenic mouse. *J Neurosci*. 2001; 21(21): 8370-7. doi: 10.1523/JNEUROSCI.21-21-08370.2001.
  9. Kloesch B, Becker T, Dietersdorfer E, Kiener H, Steiner G. Anti-inflammatory and apoptotic effects of the polyphenol curcumin on human fibroblast-like synoviocytes. *Int Immunopharmacol*. 2013; 15(2): 400-5. doi: 10.1016/j.intimp.2013.01.003.
  10. Thangapazham RL, Sharma A, Maheshwari RK. Beneficial role of curcumin in skin diseases. *Adv Exp Med Biol*. 2007; 595: 343-57. doi: 10.1007/978-0-387-46401-5\_15.
  11. Anand P, Kunnumakkara AB, Newman RA, Aggarwal BB. Bioavailability of curcumin: problems and promises. *Mol Pharmaceutics*. 2007; 4(6): 807-18. doi: 10.1021/mp70113r.
  12. Chin D, Huebbe P, Pallau K, Rimbach G. Neuroprotective properties of curcumin in Alzheimer's disease—merits and limitations. *Curr Med Chem*. 2013; 20(32): 3955-85. doi: 10.2174/09298673113209990210.
  13. Aggarwal BB, Yuan W, Li S, Gupta SC. Curcumin-free turmeric exhibits anti-inflammatory and anticancer activities: identification of novel components of turmeric. *Molecular Nutrition Food Res*. 2013; 57(9): 1529-42. doi: 10.1002/mnfr.201200838.
  14. Bisht S, Feldmann G, Soni S, Ravi R, Karikar C, Maitra A. Polymeric nanoparticle-encapsulated curcumin ('nanocurcumin'): a novel strategy for human cancer therapy. *J Nanobiotechnol*. 2007; 5: 1-18.
  15. Ang LF, Darwis Y, Por LY, Yam MF. Microencapsulation curcuminoids for effective delivery in pharmaceutical application. *Pharmaceutics*. 2019; 11(9): 451-80. doi: 10.3390/pharmaceutics11090451.
  16. Santos MB, da Costa NR, Garcia-Rojas EE. Interpolymeric complexes formed between whey proteins and Biopolymers: delivery systems of bioactive ingredients. *Compr Rev Food Sci Food Saf*. 2018; 17(3): 792-805. doi: 10.1111/1541-4337.12350.
  17. Mohammadian M, Salami M, Alavi F, Momen S, Emam-Djomeh Z, Moosavi-Movahedi AA. Fabrication and characterization of curcumin-loaded complex coacervates made of gum arabic and whey protein nanofibrils. *Food Biophys*. 2019; 14(4): 425-36. doi: 10.1007/s11483-019-09591-1.
  18. Shahgholian N, Rajabzadeh G. Fabrication and characterization of curcumin-loaded albumin/gum arabic coacervate. *Food Hydrocoll*. 2016; 59: 17-25. doi: 10.1016/j.foodhyd.2015.11.031.
  19. Tan C, Xie J, Zhang X, Cai J, Xia S. Polysaccharide-based nanoparticles by chitosan and gum arabic polyelectrolyte complexation as carriers for curcumin. *Food Hydrocoll*. 2016; 57: 236-45. doi: 10.1016/j.foodhyd.2016.01.021.
  20. Xie H, Xiang C, Li Y, Wang L, Zhang Y, Song Z, *et al.* Fabrication of ovalbumin/k-carrageenan complex nanoparticles as a novel carrier for curcumin delivery. *Food Hydrocoll*. 2019; 89: 111-21. doi: 10.1016/j.foodhyd.2018.10.027.
  21. Huang W, Wang L, Wei Y, Cao M, Xie H, Wu D. Fabrication of lysozyme/k-carrageenan complex nanoparticles as a novel carrier to enhance the stability and *in vitro* release of curcumin. *Int J Biol Macromol*. 2020; 146: 444-52. doi: 10.1016/j.ijbiomac.2020.01.004.
  22. Deka C, Aidew L, Devi N, Buragohain AK, Kakati DK. Synthesis of curcumin-loaded chitosan phosphate nanoparticle and study of its cytotoxicity and antimicrobial activity. *J Biomater Sci Polym Ed*. 2016; 27(16): 1659-73. doi: 10.1080/09205063.2016.1226051.
  23. Das RK, Kasoju N, Bora U. Encapsulation of curcumin in alginate-chitosan-pluronic composite nanoparticles for delivery to cancer cells. *Nanomend Nanotechnol Biol Med*. 2010; 6(1): 153-60. doi: 10.1016/j.nano.2009.05.009.
  24. Phongpaichit S, Nikom J, Rungjindamai N, Sakayaroj J, Hutadilok-Towatana NT, Rukachaisirikul V, *et al.* Biological activities of extracts from endophytic fungi isolated from *Garcinia* plants. *FEMS Immunol Med Microbiol*. 2007; 51(3): 517-25. doi: 10.1111/j.1574-695X.2007.00331.x.
  25. Queiroz MF, Melo KRT, Sabry DA, Sasaki GL, Rocha HAO. Does the use of chitosan contribute to oxalate kidney stone formation? *Mar Drugs*. 2015; 13(1): 141-58.
  26. Malesu VK, Sahoo D, Nayak PL. Chitosan-Sodium Alginate nanocomposites blended with cloisite 30B as a novel drug delivery system for anticancer drug curcumin. *Int. j. appl. Biol Pharm Tech*. 2011; 2(3): 402-411.
  27. Pramanik N, Mishra D, Banerjee I, Maiti TK, Bhargava P, Pramanik P. Chemical synthesis, characterization, and biocompatibility study of hydroxyapatite/chitosan phosphate nanocomposite for bone tissue engineering applications. *Int J Biomater*. 2009; 2009: 1-8. doi: 10.1155/2009/512417.
  28. Xie H, Zhang S, Li S. Chitin and chitosan dissolved in ionic liquids as reversible sorbents of CO<sub>2</sub>. *Green Chem*. 2006; 8(7): 630-3. doi: 10.1039/b517297g.
  29. Sarika PR, James NR, Kumar PRA, Raj DK. Galactosylated alginate-curcumin micelles for enhanced delivery of curcumin to hepatocytes. *Int J Biol Macromol*. 2016; 86: 1-9. doi: 10.1016/j.ijbiomac.2016.01.037.
  30. Vanderberg GW, Noue JDN. Evaluation of protein release from chitosan-alginate microcapsules produced using external or internal gelation. *J Microencapsul*. 2001; 18(4): 433-41. doi: 10.1080/02652040010019578.
  31. Zhang Y, Wei W, Lv P, Wang L, Ma G. Preparation and evaluation of alginate-chitosan microspheres for oral delivery of insulin. *Eur J Pharm Biopharm*. 2011; 77(1): 11-9. doi: 10.1016/j.ejpb.2010.09.016.
  32. Coppi G, Iannuccelli V, Leo E, Bernabei MT, Cameroni R. Chitosan-alginate microparticles as a protein carrier. *Drug Dev Ind Pharm*. 2001; 27(5): 393-400. doi: 10.1081/DDC-100104314.

**Cite this article:** Sarma A, Deka C, Devi SP, Kakati DK. Synthesis of Curcumin-Loaded Complex Coacervate of Chitosan Phosphate and Sodium Alginate and Study of their Antibacterial Activity. *Indian J of Pharmaceutical Education and Research*. 2024;58(2s):s420-s428.